Nonequilibrium pattern formation in circularly confined two-dimensional systems with competing interactions

X. B. Xu,* T. Tang, Z. H. Wang, X. N. Xu, G. Y. Fang, and M. Gu
Collaborative Innovation Center of Advanced Microstructures, School of Physics, Nanjing University, Nanjing 210093, People's Republic of China

(Received 23 October 2020; accepted 19 December 2020; published 8 January 2021)

We numerically investigate the nonequilibrium behaviors of classic particles with competing interactions confined in a two-dimensional logarithmic trap. We reveal a quench-induced surprising dynamics exhibiting rich dynamic patterns depending upon confinement strength and trap size, which is attributed to the time-dependent competition between interparticle repulsions and attractions under a circular confinement. Moreover, in the collectively diffusive motions of the particles, we find that the emergence of dynamic structure transformation coincides with a diffusive mode transition from superdiffusion to subdiffusion. These findings are likely useful in understanding the pattern selection and evolution in various chemical and biological systems in addition to modulated systems, and add a new route to tailoring the morphology of pattern-forming systems.

DOI: 10.1103/PhysRevE.103.012604

I. INTRODUCTION

The systems with competing interactions exhibit a set of interesting equilibrium and nonequilibrium structures showing spatial modulation, a periodic deviation or deformation of one basic structure with space-group symmetry, which has attracted a large amount of experimental and theoretical attention [1–3]. In equilibrium, the presence of regular spatial patterns is attributed to a compromise of competing interactions [4–13]. That is, the formation of discrete clusters is induced by short-range attractions, and the long-range ordering of a modulated structure is stabilized by interparticle repulsions. It has been established that, for a certain particle-particle interaction potential, particle density will become an exact controlling parameter for the formation of modulated structures [10,11]. With increasing particle density, two-dimensional (2D) modulated systems form ordered clumps and stripes consisting of internally ordered particles, anticlumps surrounded by hexagonally arranged particles, and an ordered particle lattice [4,10,11]. In the three-dimensional (3D) case, modulated systems show the following sequence of ordered phases with increasing volume fraction of particles: spherical clusters, cylindrical clusters, gyroid network of particles, layers of particles, gyroid network of voids, cylindrical voids and spherical voids [14–17]. In nonequilibrium, it has been found that modulated systems can also form various dynamical structures or patterns depending upon the previous history of the systems [6,18–21]. For example, in a moving modulated system with quenched disorders driven by external forces or fields, simulations show that depending on the magnitude of pinning force two distinct moving steady states arise at high drives [18]: For weaker pinning, the moving particles show labyrinth patterns induced by the transverse instability in the system [1,22]. For stronger pinning, the transverse modes are effectively suppressed by drives, so the particle motion becomes frozen in the direction perpendicular to the drive [23]. Consequently, the moving particles form ordered stripelike patterns.

On the other hand, new modulated structures with distinct ordering can be produced by adding a confinement or trap [14,15,24–37]. For example, in quasi-one-dimensional channel-like confinements, it has been found that the occurrence of incommensurability between the periodicity of modulated structures and the width of channel causes the structural distortion of particle clusters for minimizing the total energy [14,24,25], inducing various types of ordered structures consisting of deformed (elongated or kinked) clusters [26,27]. Moreover, for such confined systems, McDermott and coauthors show that regular metastable structures are formed by using quasistatic compression-decompression [38]. This suggests that the structural morphology of pattern formation systems can be created by a dynamic procedure. In addition to trap size, trap shape is also crucial in determining the equilibrium structures of modulated systems. In modulated systems with a circular trap, it has been numerically demonstrated that the systems form a variety of equilibrium configurations with concentric arrangements consisting of either clumps or stripes or rings [28–37]. The formation of such ringlike cluster structures is owing to the ordering competition between the confinement boundary and the ground-state structure for the corresponding infinite system, which produces a preordering structure which inherits properties from both incompatible structures [39]. In contrast to the equilibrium physical property of circularly confined modulated systems, far less is known about the corresponding nonequilibrium behaviors under varying external fields. Specially, it is unclear whether new pattern formation phenomena present and how the confinement affects the structural evolution of the systems in nonequilibrium.

*Corresponding author: xxb@nju.edu.cn

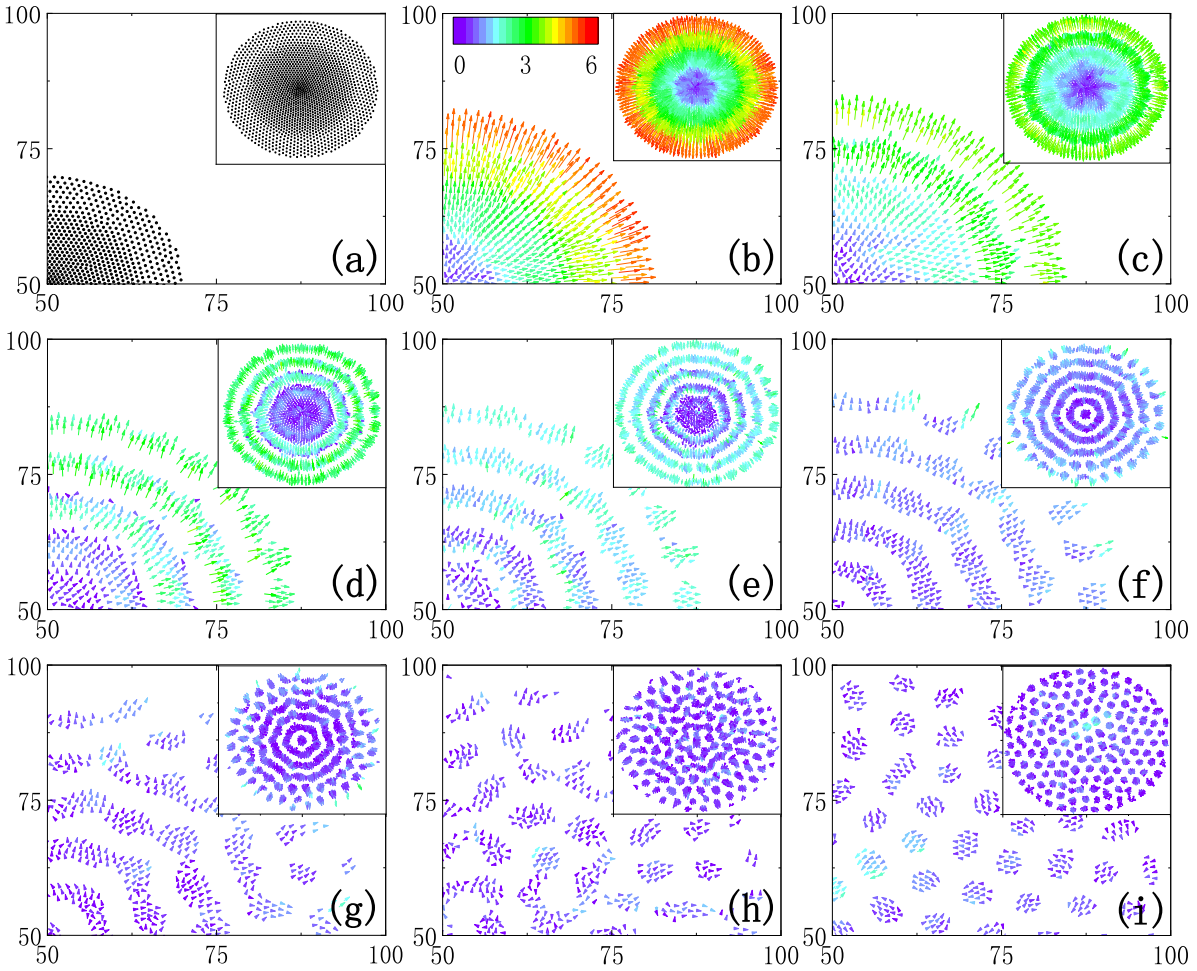

FIG. 1. Particle positions and velocities at different times for the modulated system undergoing expansion by applying a sudden jump of confinement strength from $\beta_s = 15.1$ to $\beta_f = 0.1$. Only one quarter of the sample is shown for clarity, while the inserts show the entire area. Both the color code and the arrow length indicate the magnitude of particle velocity. The arrow shows the instantaneous direction of motion, and its tail is at the particle position. The times t at which the figures were taken are as follows: (a) $t = 0$, (b) $t = 1$, (c) $t = 2$, (d) $t = 3$, (e) $t = 4$, (f) $t = 6$, (g) $t = 9$, (h) $t = 13$, and (i) $t = 100$. See Supplementary Movie S1 for a movie of the entire explosion sequence [46].

Here, we will focus on a two-dimensional modulated system confined in a circularly logarithmic trap [37]. In order to control the dynamics of modulated systems, the initial nonequilibrium state is prepared by using a rapid change or quench in the confining strength of the trap. The system then evolves toward its final equilibrium state, which is quasiordered clumps consisting of particles [37]. We reveal a novel dynamics for an equilibrium single-clump system, manifesting as various long-lasting dynamic structures including concentric particle rings, stripes, and a ringlike arrangement of clumps, as well as reticulation structures depending on confinement strength and trap size. These patterns are similar to those occurring in Coulomb and colloidal explosions [40–44]. For laser-driven atomic cluster explosion, a large number of electrons leave an atom cluster held together due to van der Waals forces, and the excess positive charge remains inside. This drives the expansion of the cluster in a hydrodynamic manner [42]. Similarly, for an aggregated colloid cluster which trapped by optical laser tweezers, by using long-range repulsive magnetic fields, a pattern of concentric rings induced by the initial shell-like ordering of the colloidshas been observed [43]. Moreover, we find that the dynamic ring-to-stripe structural transformation occurs along with a superdiffusion-to-subdiffusion mode transition in the collectively diffusive motions of the particles. These findings will provide insights into the nature of the nonequilibrium dynamics of the system.

II. SIMULATION

We consider a two-dimensional (2D) overdamped Langevin simulation of a system of pointlike particles with competing interactions confined in a circular trap. Such simulation is appropriate for systems like colloids, superconducting vortices, and magnetic domains [18]. We do not take into account possible hydrodynamic effects. The equation of motion for a particle i is

$$\eta \frac{d\mathbf{r}_i}{dt} = \mathbf{F}^{pp} + \mathbf{F}^{pt} + \mathbf{F}^{T}, \tag{1}$$

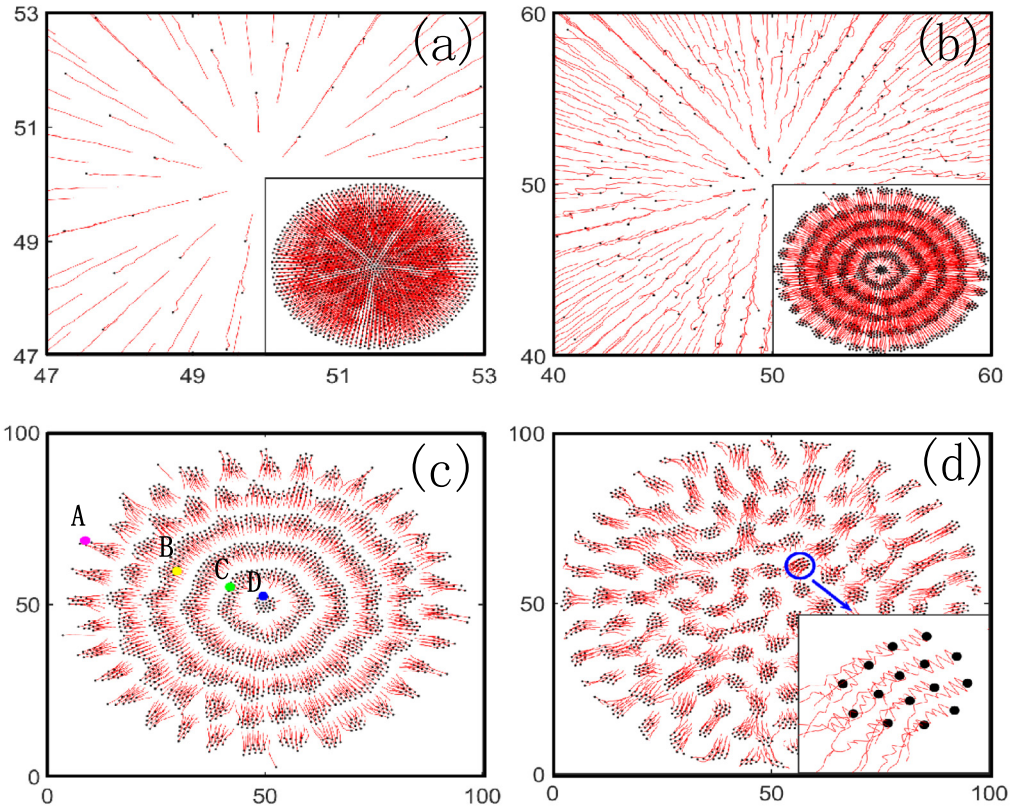

FIG. 2. The sequential trajectories with different durations t for the explosion shown in Fig 1: (a) $t = 0 \rightarrow 1$, (b) $t = 1 \rightarrow 5$, (c) $t = 5 \rightarrow 10$, and (d) $t = 10 \rightarrow 20$. In both panels (a) and (b), the central region of the sample is shown for clarity, and the inserts show the entire area. The insert in panel (d) is the enlarged plot of one local clumplike cluster. The trajectories clearly show collective motions of the particles in the clump over very short distances.

where η is the viscous drag coefficient which we set to unity, $\mathbf{F}^{pp}$ and $\mathbf{F}^{pt}$ are the forces due to particle-particle interactions and particle-trap interactions respectively, and $\mathbf{F}^{T}$ is the the thermal stochastic force. The particle-particle interaction force is given by [10]

$$F^{pp}(r_{ij}) = \frac{1}{r_{ij}^2} - Be^{-Cr_{ij}}, \tag{2}$$

where r_{ij} is the distance between particles i and j, the first term is a long-range repulsion, and the second term is a short-range attraction. The parameter B reflects the relative strength of attraction to repulsion, and the screening length $1/C$ determines the attraction range. For the competing interactions, the long-range repulsive forces (decaying with distance as $1/r^2$) studied here are due to Coulomb repulsion, while the nature of the short-range attractive forces varies between systems. For examples, in layered transition metal oxides, two holes interact through a potential which is composed of a repulsive Coulomb and two attractive exponential terms. The short-range attraction between holes is due to the short-range antiferromagnetic fluctuations [7]. In low-κ type II superconducting systems, the short-range intervortex attraction which is in exponential form arises due to the vortex core-core interaction [11]. Besides, such interaction model could be used to study colloidal as well as charged-dust systems [30]. The particles are trapped by a confinement potential with logarithmic form, which has been proposed to study the confinement effects on the phase behaviors of modulated systems [37],

$$V(r) = -\beta ln(R - r), \tag{3}$$

where β characterizes the strength (or steepness) of the confining potential, R is the radius of the confinement, and this applies only for $r < R$. Correspondingly, the trap exerts a centripetal repulsive force on the particle i, $\mathbf{F}^{pt}(r_i) = -\beta/(R - r_i)$. As compared with two typical confinements, hard-wall potentials [$V(r) = 0$ for $r < R$ and $V(r) = \infty$ for $r \geqslant R$] and soft-wall potentials including harmonic ones, this confinement model has both definite confining boundary (or size) and steepness. This confinement may appear in superconducting disks and can be artificially implemented by using an external field or by nanostructuring or etching the surface [37]. The thermal stochastic force is implemented with a Box-Müller random number generator and has properties $\langle F_i^{\mathrm{T}} \rangle = 0$ and $\langle F_i^{\mathrm{T}}(t) F_j^{\mathrm{T}}(t') \rangle = 2\eta k_{\mathrm{B}} T \delta_{ij} \delta(t - t')$ at a given temperature T. We normalize lengths by l_0, forces by f_0, and time by $\tau = \eta l_0 / f_0$. The equation of motion is integrated by an Euler scheme with a normalized time step of $\Delta t = 0.001$. We use an efficient method to calculate the long-range Coulomb repulsion by cutting off the interaction potential smoothly [45]. We let the cutoff radius $R_c = 7.5a_0$, where a_0 is the hexagonal lattice constant for the same particle density. For $R_c > 7.5a_0$, similar results are obtained. We employ the

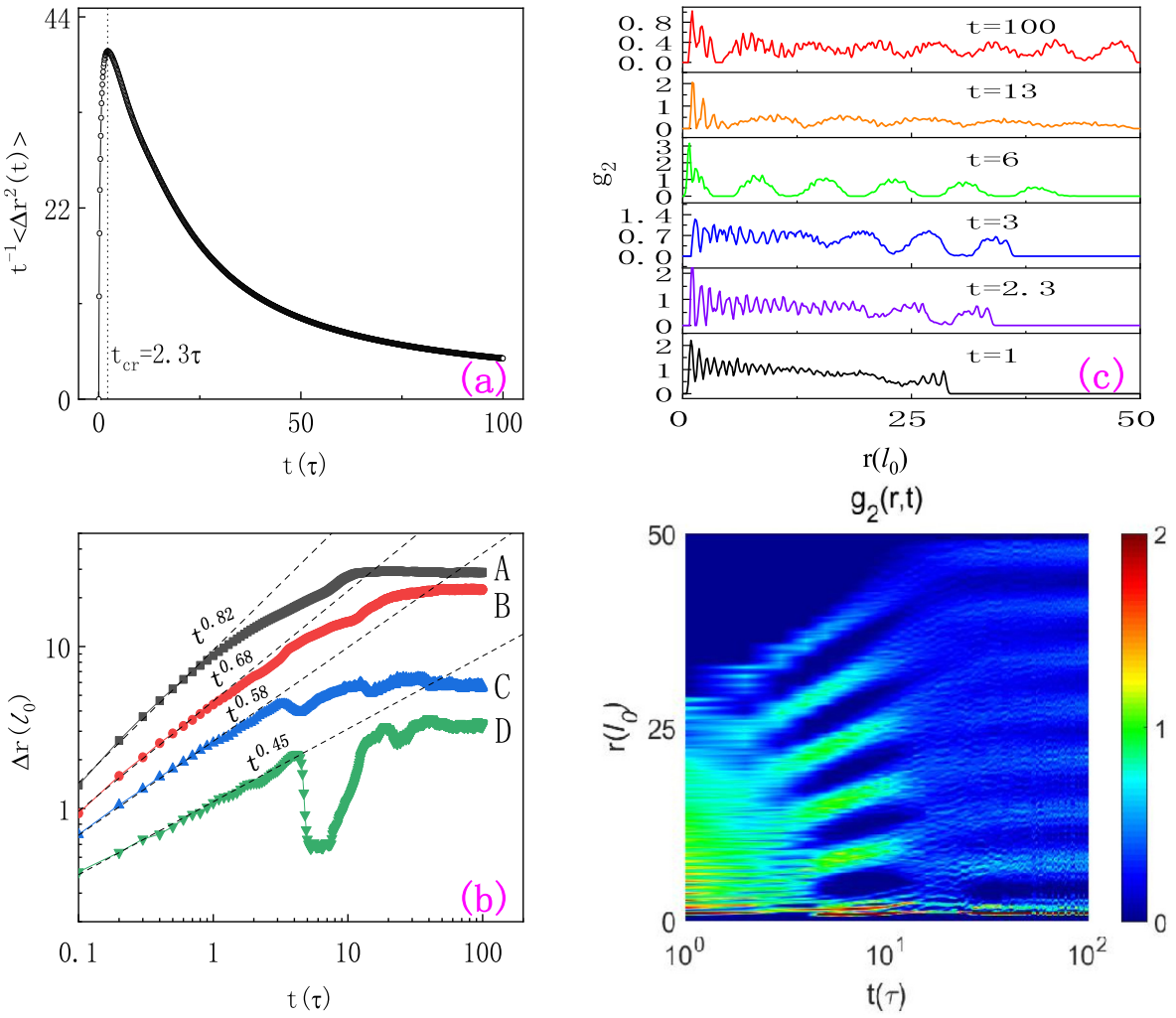

FIG. 3. Temporal and spatial characterization of the explosion dynamics of the modulated system. (a) Time evolution of mean-squared displacement scaled by the time shows a diffusion crossover from superdiffusive to subdiffusive behaviors at $t_{tr} = 2.3\tau$. (b) Time evolution of the displacements for four selected particles labeled A, B, C, and D in Fig. 2(c). (c) The radial distribution function $g_2(r)$ of the particle distributions at different times. (d) Time-space plot of average radial density.

total particle number $N_p = 1936$ (for a smaller trap size R, similar results are obtained with a smaller particle number N), $R = 50$ (unless specified otherwise), $l_0 = 7 \times 10^{-8}$ m, $f_0 = 2 \times 10^{-12}$ N, $\tau = 3.5 \times 10^4$ s, $B = 2$, and $C = 1$. The initial state of the system is obtained by using a static annealing scheme at a fixed value of confinement strength and trap size ($\beta_s = 15.1$ and $R = 50$). First the particles are put randomly on a circle box centered at the origin. Then the system is annealed from a high temperature, which is set to a value well above the melting temperature displayed by the system, to zero temperature in a small annealing rate, and finally forms an equilibrium single-clump cluster consisting of the particles [37]; see the inset of Fig. 1(a).

III. RESULTS AND DISCUSSION

We first investigate, by tracking the particle motions, the microscopic process of the modulated system which undergoes "explosion" in the presence of an abrupt decrease of confinement strength from $\beta_s = 15.1$ to $\beta_f = 0.1$ without delay. As illustrated in Figs. 1(a)–1(i), we present the particle positions and velocities at different times. Figures 2(a)–2(d) shows the sequential trajectories with different durations. The entire explosion sequence can be seen in Supplementary Movie S1 [46]. It can be found that the system shows a rich variety of patterns, which is already the case in equilibrium [37]. Clearly, the existence of multiple length scales in the interparticle interaction is crucial for the formation of these structures. The overall interaction force includes not just two opposite ranges of interactions but three, namely the (very) short-range repulsion, intermediate range of attraction, and long-range repulsion. These ranges are strongly dependent on the balance of original repulsion and attraction governed by the constants B and C. The fact that the particles do not have a finite size but are considered pointlike implies that they can experience all three ranges.

We find that the explosion dynamics can be characterized by three stages. The early stage corresponds to the emergence

of expanding concentric rings (particles are organized in different rings around the center): At $t = 0$ in Fig. 1(a), the system forms the initial equilibrium state for $\beta = 15.1$, i.e., a single dense bubblelike cluster structure. After the quench of confinement strength, it can be found that almost all particles (except a few particles nearby the trap center) move quickly outward along the radial direction due to the interparticle repulsions in a very short range [see Fig. 1(b) ($t = 1$)] and form expanding concentric rings [see Fig. 2(a)]. This is reminiscent of the patterns observed in Coulomb explosions [40,41] and in colloidal explosions [43,44]. For the sake of simplicity, similarly, one can temporally refer to the explosion of modulated systems (which are sometimes termed as mermaid systems) as "mermaid explosion" [47].

The intermediate stage corresponds to the continuous formation of expanding concentric stripelike clusters. Figure 1(c) for $t = 2$ shows that one ringlike stripe forms in the outermost layer of the expanding cluster structure. This suggests that the interparticle attractions become important for the relating particles with increasing particle separations. As a result, particle layering occurs and manifests as the emergence of centripetal movements (in the opposite direction of expansion) for some particles; see the particle trajectories in Fig. 2(b). It is worth emphasizing that the formation of expanding concentric stripes is the signature for mermaid explosions, in contrast with the expanding concentric rings for colloidal explosions [43,44]. For further expansion, the system forms more ringlike stripes with concentric configurations, as shown in Figs. 1(d)–1(f), for $t = 3$, $t = 4$, and $t = 6$, respectively. The outermost stripe transitions gradually into a circular arrangement of clumps due to the decrement of local particle densities.

The late stage corresponds to the structure transformation from a cluster consisting of concentric stripes and ringlike arrangement of clumps into quasiordered clumps through an order-disorder transition mechanism. It is seen that both the intrastripe and interstripe particle interactions become weak with the expansion. In this case, even small transverse instabilities or force fluctuations can make particles move out of the caging well formed by the nearest neighbors. As a result, obvious transverse motions arise and manifest as twisting or stretching or breaking in the stripes, as illustrated in Fig. 1(g) ($t = 9$), but either deformed stripes or clumps are still organized in different rings around the center. With further expansion, the ringlike arrangements will be completely broken by transverse instabilities and the system structure gradually evolves into polydisperse domains consisting of discrete clumps and interconnected and irregular stripes, as shown in Fig. 1(h) ($t = 13$). Then the system undergoes a slow structural relaxation toward its equilibrium state; see Fig. 1(i) ($t = 100$). Besides, our simulations show that the ordering of clumps is not synchronized with intraclump particles. From the particle trajectories for $t = 10 \rightarrow 20$ in Fig. 2(d), one can find that the clumps move irregularly, while the intraclump particles show interesting coherently oscillating motions [see the insert of Fig. 2(d)]. This is due to the fact that the short-range repulsions between intraclump particles are always dominant over the long-range repulsions for interclump particles, leading to a relatively short relaxation time for the intraclump particles to reach their equilibrium ordered distributions.

To quantitatively investigate the explosion dynamics of the modulated system, we calculate four time- and space-dependent functions: (i) the particle mean-squared displacement (MSD) $\langle \triangle r^2(t) \rangle = (1/N) \sum_{i=1}^{N} |r^2(t) - r^2(t_0)|$, characterizing the dynamic property of particles in the relaxation (diffusion) process, (ii) the displacement for particle i, $\Delta r_i(t) = |r_i(t) - r_i(0)|$, characterizing the motion of the specifically selected particles, (iii) the radial distribution function (RDF) $g_2(r) = \frac{\pi R^2}{N} \frac{\Delta N}{2\pi r \Delta r}$, where ΔN is the number of particles whose distance to the origin point is between r and $r + \Delta r$, characterizing the layering properties of the dynamical structures [48], and (iv) the radial density $\rho(r)$, characterizing the average number density of the particles whose distance to the origin point is between r and $r + \Delta r$, which can be determined by using the relation $\rho(r) = g_2(r) \frac{N}{\pi R^2}$.

It is a standard forced diffusion that the motion of the particles in an equilibrium single-clump modulated system with high density undergoing expansion toward the "vacuum" region in the trap [49]. Basically, the globally driving effect induced by changing the external confining potential can lead to superdiffusive behaviors [50–53]. While the intrinsic viscosity of the system and the confining effect via the trap will

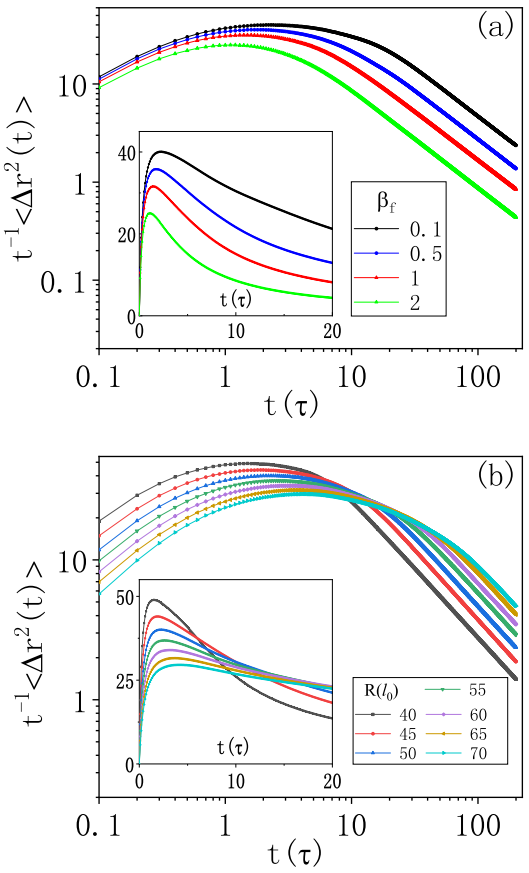

FIG. 4. Time evolution of mean-squared displacement scaled by the time in log-log plot and linear plot (insert): (a) for different confinement strengths β_f at $R = 50$ and $\beta_s = 15.1$; (b) for different trap sizes R at $\beta_s = 15.1$ and $\beta_f = 0.1$.

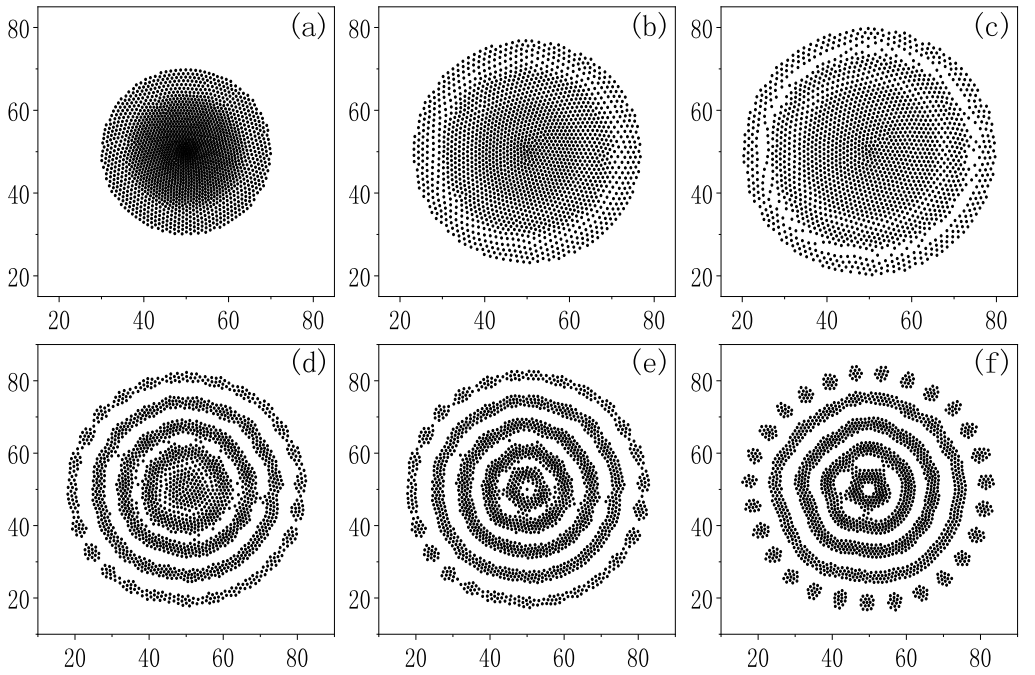

FIG. 5. Particle positions at different times for the modulated system undergoing expansion by applying a sudden jump of confinement strength from $\beta_s = 15.1$ to $\beta_f = 2$ at $R = 50$: (a) $t = 0$, (b) $t = 1$, (c) $t = 2$, (d) $t = 5$, (e) $t = 7$, and (f) $t = 200$. See Supplementary Movie S2 for a movie of the entire explosion sequence [46].

produce subdiffusive behaviors [50,51,54,55]. Clearly, the diffusive behaviors of the expanding system are governed by the interplay between these effects. This leads to a diffusion mode transition from superdiffusion to subdiffusion at $t_{\rm tr} = 2.3\tau$ [see Fig. 3(a)], where $t_{\rm tr}$ is the transition time.

On the other hand, the system displays highly dynamic density inhomogeneity and remarkable instability in the explosion; see Fig. 2. Naturally, it is expected that the obviously dynamic disparities arise for different particles depending on their relative positions in the initial single-clump structure, so we measure the displacements $\Delta r(t)$ of four selected particles located at representative positions of the cluster structure, labeled A, B, C, and D, as shown in Fig. 2(c). In Fig. 3(b), for particles A, B, and C, following an initial superdiffusive regime, we find the particles exhibit subdiffusive behaviors in the long time. For particle A, for $t < 1\tau$, the $\Delta r(t)$ shows a power-law dependence on the time $\Delta r(t) \sim t^{\alpha}$, $\alpha = 0.82$, where α describes the particle diffusibility. Similarly, the $\Delta r(t)$ for the particles B and C also show a power-law dependence on the time with $\alpha = 0.68$ and $\alpha = 0.58$, respectively. In contrast with particle A, which locates at the outermost layer of the cluster structure, the existence of stronger caging effect decreases the particle diffusibility of the particles B and C. For particle D, which locates in the central area of the trap, $\Delta r(t)$ shows the subdiffusive behaviors even in the short time because of the strong caging effect. For $4\tau < t < 5\tau$, $\Delta r(t)$ shows a rapid decrement with time. This is attributed to the occurrence of particle centripetal movement [see Fig. 2(b)] due to the instantaneously dominant short-range attractions in the formation of a clumplike cluster at the trap center. Moreover, the rapid increment of $\Delta r(t)$ with time for $7.5\tau < t < 19\tau$ reflects the enhanced particle motility during the stripe-clump transformation process.

Figure 3(c) shows the radial distribution function $g_2(r)$ of the particle distributions at different times. At $t = 1\tau$, we can find a series of peaks occur in the $g_2(r)$ for $r \leqslant 29.25l_0$, indicating the layer ordering of the particles in the early stage of the explosion. At $t = 2.3\tau$, a main peak with several subpeaks presents at $r = 32$, which is a signal of the formation a circular stripe in the edge of the expanding cluster. The three peaks for $15.75l_0 < r < 36.3l_0$, at $t = 3\tau$, correspond to the concentric and ringlike stripes in the intermediate stage of the explosion [see Fig. 1(d)]. While three subpeaks occur in the outermost main peak (at $r \approx 34.2l_0$), indicating the intrastripe particles form ringlike distributions. The $g_2(r)$ for $t = 6\tau$ shows six main peaks with near equidistance, which are respectively produced by five concentric stripes or circular arrangements of clumps and a central clump [see Fig. 1(f)]. Note that these main peaks in $g_2(r)$ are smoothed at $t = 13\tau$. This indicates the formation of disordered clumps in the stripe-to-clump structure transformation in the late stage of the explosion, as shown in Fig. 1(h). The $g_2(r)$ for $t = 100\tau$ displays the reappearance of multiple main peaks with various subpeaks, signaling the formation of quasiordered clumps with circular arrangements [see Fig. 1(i)]. Furthermore, we obtain the spatiotemporal evolution of the $g_2(r, t)$ of the moving particles, as shown in Fig. 3(d). In addition to capturing the structural transition of the locations of the high- and low-density regions in the spatiotemporal structure, it consistently confirms the arrangements of particle rings, particle stripes, and the ringlike distributions of particle clumps are periodic in different stages of the explosion. In the short-time regime, $g_2(r, t)$ demonstrates homogeneously and continuously layered distributions, reflecting the ordering of the dynamic structures in the early stage of the explosion. In the intermediate-time regime, $g_2(r, t)$ shows five bright stripes that mark the

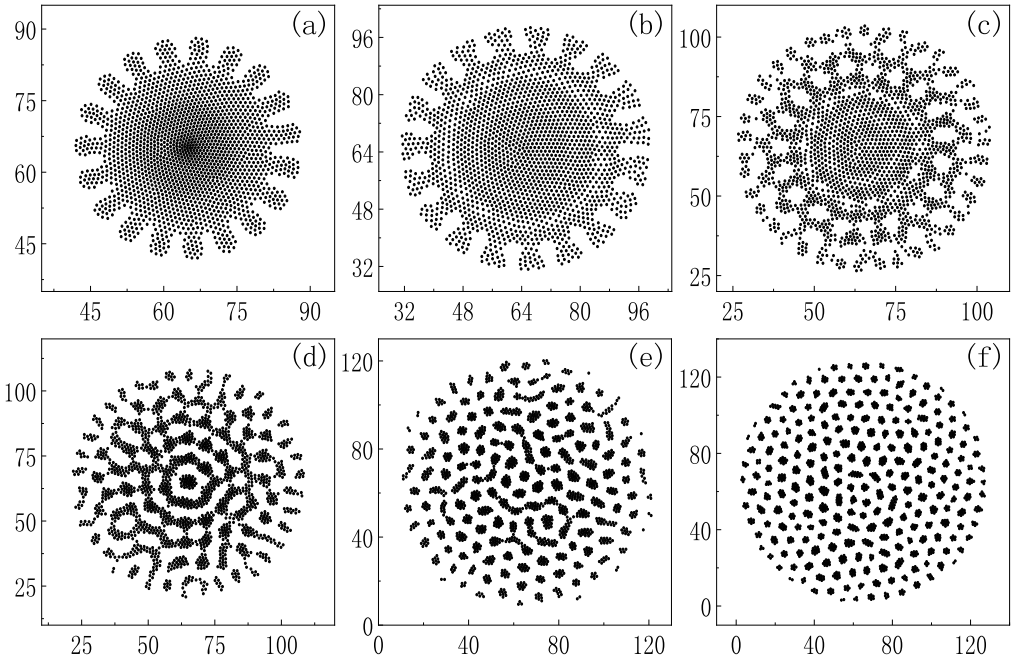

FIG. 6. Particle positions at different times for the modulated system undergoing expansion by applying a sudden jump of confinement strength from $\beta_s = 15.1$ to $\beta_f = 0.1$ at $R = 65$: (a) $t = 0$, (b) $t = 2$, (c) $t = 3$, (d) $t = 6$, (e) $t = 20$, and (f) $t = 200$. See Supplementary Movie S3 for a movie of the entire explosion sequence [46].

formation and evolution of the expanding stripes. Before entering the long-time regime corresponding to the occurrence of seven stripes, the five stripes are blurred, reflecting the structure evolution during the early stage of order-disorder development.

In view of the fact that the confining effect plays an important role in this quench-induced dynamics, now we measure the time evolution of MSD scaled by the time for different confinement strengthes β_f and trap sizes R, as shown in Fig. 4. It is seen that the particle diffusibility should be enhanced with decreasing β_f. In this case, the superdiffusion duration will become longer before entering the subdiffusion regime. Accordingly, the time-scaled MSD peaks shift toward the longer time regimes with the decrement of β_f; see the inserts of Figs. 4(a). For increasing R, at fixed confinement strength β_s, it is clear that the corresponding initial equilibrium systems are of lower particle densities. This implies smaller short-range interparticle repulsions and thus lower diffusibility in the short time. As a result, the time-scaled MSD peaks shift toward the shorter time regimes with the decrement of R, as shown in Figs. 4(b). On the other hand, in the long time, the confining interactions are decreasing with the increment of trap size R, leading to enhanced particle diffusibility, as demonstrated in Fig. 4(b). Additionally, in the long time, the MSDs exhibit nearly a power-law dependence on the time either for different β_f or for different R; see Figs. 4(a) and 4(b), respectively.

In addition to the diffusive behaviors, our simulations show that the varying confinement parameters have an obvious influence on the dynamic phase behaviors of the system. This manifests as distinct features in the structural evolutions in explosions from those shown in the typical explosion as demonstrated in Fig. 1. For examples, for a larger β_f, say $\beta_f = 2$, the expanding system only displays two kinds of dynamic structures including expanding particle rings [see Figs. 5(a) and 5(b) at at the early stage] and expanding circular stripes with or without a ringlike arrangement of clumps [see Figs. 5(c)–5(f) at the late stage]. The entire explosion sequence can be seen in Supplementary Movie S2 [46]. While for large R, say $R = 65$, the initial state of the system shows a gear-like cluster with fringed outer rims evenly arranged along the circumference, as shown in Fig. 6(a). In this case, the Coulomb-type explosion patterns can be observed in the internal part of the cluster structure with higher particle densities; see Fig. 6(b). Then these dynamic particle rings transition into expanding circular stripes with the explosion, as shown in Figs. 6(c) and 6(d), while the rims in the edge transform gradually into a complex reticulation structure with nearly homogeneous voids through expanding and bifurcating in the explosion [see Figs. 6(b) and 6(c)]. This suggests that history or memory effect plays an important role in the pattern selection and evolution of the system, which also indicates new directions for future investigations. The entire explosion sequence for the initial gear-like cluster can be seen in Supplementary Movie S3 [46].

IV. CONCLUSION

In conclusion, we numerically study the nonequilibrium behaviors of classic particles with competing interactions confined in a two-dimensional logarithmic trap. We reveal a quench-induced dynamics for an equilibrium single-clump system undergoing expansion, displaying various dynamic structures manifesting as persistent dynamic rings,

circular stripes, and a ringlike arrangement of clumps, as well as reticulation structures depending on confinement strength and trap size. These are attributed to the time-dependent competition between interparticle repulsions and attractions under a circular confinement. Moreover, in the collectively diffusive motions of the particles, our simulations show that the emergence of dynamic structural transformation coincides with a diffusive mode transition from superdiffusion to subdiffusion. Our work could prove useful in understanding the pattern selection and evolution in various chemical and biological systems in addition to modulated systems [1,22,56] and add a possible route to tailoring the morphology of pattern forming systems by using explosion protocols.

ACKNOWLEDGMENTS

X.B. thank S. Y. Ding for helpful discussions. This work was supported by a grant from the National Basic Research Program of China (Grant No. 2016YFA0201604).

[1] R. C. Desai and R. Kapral, *Dynamics of Self-Organized and Self-Assembled Structures* (Cambridge University Press, Cambridge, UK, 2009).
[2] M. Seul and D. Andelman, Science **267**, 476 (1995).
[3] D. Andelman and R. E. Rosensweig, J. Phys. Chem. B **113**, 3785 (2009).
[4] C. Roland and R. C. Desai, Phys. Rev. B **42**, 6658 (1990).
[5] L. Q. Chen and A. G. Khachaturyan, Phys. Rev. Lett. **70**, 1477 (1993).
[6] C. Sagui and R. C. Desai, Phys. Rev. E **49**, 2225 (1994).
[7] B. P. Stojković, Z. G. Yu, A. R. Bishop, A. H. Castro Neto, and N. Grønbech-Jensen, Phys. Rev. Lett. **82**, 4679 (1999).
[8] C. J. Olson Reichhardt, C. Reichhardt, and A. R. Bishop, Phys. Rev. Lett. **92**, 016801 (2004).
[9] L. Komendová, M. V. Milošević, and F. M. Peeters, Phys. Rev. B **88**, 094515 (2013).
[10] C. J. Olson Reichhardt, C. Reichhardt, and A. R. Bishop, Phys. Rev. E **82**, 041502 (2010).
[11] X. B. Xu, H. Fangohr, S. Y. Ding, F. Zhou, X. N. Xu, Z. H. Wang, M. Gu, D. Q. Shi, and S. X. Dou, Phys. Rev. B **83**, 014501 (2011).
[12] X. B. Xu, H. Fangohr, M. Gu, W. Chen, Z. H. Wang, F. Zhou, D. Q. Shi, and S. X. Dou, J. Phys.: Condens. Matter **26**, 115702 (2014).
[13] E. O. Lima, P. C. N. Pereira, H. Löwen, and S. W. S. Apolinario, J. Phys.: Condens. Matter **30**, 325101 (2018).
[14] N. G. Almarza, J. Pękalski, and A. Ciach, Soft Matter **12**, 7551 (2016).
[15] J. Pękalski, E. Bildanau, and A. Ciach, Soft Matter **15**, 7715 (2019).
[16] Y. Zhuang, K. Zhang, and P. Charbonneau, Phys. Rev. Lett. **116**, 098301 (2016).
[17] H. Serna, E. G. Noya, and W. T. Góźdź, Langmuir **35**, 702 (2019).
[18] C. Reichhardt, C. J. Olson Reichhardt, I. Martin, and A. R. Bishop, Phys. Rev. Lett. **90**, 026401 (2003).
[19] C. Reichhardt, C. J. Olson, I. Martin, and A. R. Bishop, Europhys. Lett. **61**, 221 (2003).
[20] C. J. Olson Reichhardt, C. Reichhardt, I. Martin, and A. R. Bishop, Physica D (Amsterdam, Neth.) **193**, 303 (2004).
[21] X. B. Xu, H. Fangohr, Z. H. Wang, M. Gu, S. L. Liu, D. Q. Shi, and S. X. Dou, Phys. Rev. B **84**, 014515 (2011).
[22] M. C. Cross and P. C. Hohenberg, Rev. Mod. Phys. **65**, 851 (1993).
[23] T. Giamarchi and P. Le Doussal, Phys. Rev. Lett. **76**, 3408 (1996).
[24] A. Imperio and L. Reatto, Phys. Rev. E **76**, 040402(R) (2007).
[25] A. J. Archer, Phys. Rev. E **78**, 031402 (2008).
[26] D. McDermott, C. J. Olson Reichhardt, and C. Reichhardt, Soft Matter **10**, 6332 (2014).
[27] C. A. Wei, X. B. Xu, X. N. Xu, Z. H. Wang, and M. Gu, Physica C (Amsterdam, Neth.) **548**, 55 (2018).
[28] K. Nelissen, B. Partoens, and F. M. Peeters, Phys. Rev. E **71**, 066204 (2005).
[29] F. F. Munarin, K. Nelissen, W. P. Ferreira, G. A. Farias, and F. M. Peeters, Phys. Rev. E **77**, 031608 (2008).
[30] Y. H. Liu, L. Y. Chew, and M. Y. Yu, Phys. Rev. E **78**, 066405 (2008).
[31] Y. H. Liu, Z. Y. Chen, M. Y. Yu, and A. Bogaerts, Phys. Rev. E **74**, 056401 (2006).
[32] Y. H. Liu, B. X. Chen, and L. Wang, Chin. Phys. Lett. **23**, 1540 (2006).
[33] Y. H. Liu and Z. Y. Chen, J. Phys.: Condens. Matter **19**, 356213 (2007).
[34] L. Q. Costa Campos, C. C. de Souza Silva, and S. W. S. Apolinario, Phys. Rev. E **86**, 051402 (2012).
[35] L. Q. Costa Campos, S. W. S. Apolinario, and H. Löwen, Phys. Rev. E **88**, 042313 (2013).
[36] L. Q. Costa Campos and S. W. S. Apolinario, Phys. Rev. E **91**, 012305 (2015).
[37] X. B. Xu, Z. H. Wang, X. N. Xu, G. Y. Fang, and M. Gu, J. Chem. Phys. **152**, 054906 (2020).
[38] D. McDermott, C. J. Olson Reichhardt, and C. Reichhardt, Soft Matter **12**, 9549 (2016).
[39] T. Neuhaus, M. Marechal, M. Schmiedeberg, and H. Löwen, Phys. Rev. Lett. **110**, 118301 (2013).
[40] H. Wabnitz, L. Bittner, A. R. B. De Castro, R. Döhrmann, P. Gürtler, T. Laarmann, W. Laasch, J. Schultz, A. Swiderski, K. Von Haeften, T. Möller, B. Faatz, A. Fateev, J. Feldhaus, C. Gerth, U. Hahn, E. Saldin, E. Schneidmiller, K. Sytchev, K. Tiedtke, R. Treusch, and M. Yurkov, Nature (London) **420**, 482 (2002).
[41] A. E. Kaplan, B. Y. Dubetsky, and P. L. Shkolnikov, Phys. Rev. Lett. **91**, 143401 (2003).
[42] T. Ditmire, Phys. Rev. A **57**, R4094 (1998).
[43] A. V. Straube, A. A. Louis, J. Baumgartl, C. Bechinger, and R. P. A. Dullens, Europhys. Lett. **94**, 48008 (2011).
[44] A. V. Straube, R. P. A. Dullens, L. S. Geier, and A. A. Louuis, J. Chem. Phys. **139**, 134908 (2013).

[45] H. Fangohr, A. Price, S. Cox, P. A. J. de Groot, G. J. Daniell, and K. S. Thomas, J. Comput. Phys. **162**, 372 (2000).
[46] See Supplemental Material at http://link.aps.org/supplemental/10.1103/PhysRevE.103.012604 for the modulated system undergoing expansion by applying a sudden jump of confinement strength: Movie S1, from $\beta_s = 15.1$ to $\beta_f = 0.1$ at $R = 50$; Movie S2, from $\beta_s = 15.1$ to $\beta_f = 2$ at $R = 50$; and Movie S3, from $\beta_s = 15.1$ to $\beta_f = 0.1$ at $R = 65$.
[47] C. P. Royall, Soft Matter **14**, 4020 (2018).
[48] H. J. Zhao, V. R. Misko, and F. M. Peeters, New J. Phys. **14**, 063032 (2012).
[49] I. M. Sokolov, Soft Matter **8**, 9043 (2012).
[50] J. H. Jeon, A. V. Chechkin, and R. Metzler, Phys. Chem. Chem. Phys. **16**, 15811 (2014).
[51] E. Hatta, J. Phys. Chem. B **112**, 8571 (2008).
[52] X. Q. Shi and Y. Q. Ma, Nat. Commun. **4**, 3013 (2013).
[53] H. E. Ribeiro and F. Q. Potiguar, Physica A (Amsterdam, Neth.) **462**, 1294 (2016).
[54] A. S. Bodrova, A. V. Chechkin, A. G. Cherstvy, H. Safdari, I. M. Sokolov, and R. Metzler, Sci. Rep. **6**, 30520 (2016).
[55] V. O. Kharchenko and I. Goychuk, Phys. Rev. E **87**, 052119 (2013).
[56] A. J. Koch and H. Meinhardt, Rev. Mod. Phys. **66**, 1481 (1994).